



Published in final edited form as:

Immunol Cell Biol. 2009 July ; 87(5): 419–427. doi:10.1038/icb.2009.2.

Ontogeny and Phagocytic Function of Baboon Lung Dendritic Cells

Shanjana Awasthi^{*†}, Roman Wolf[‡], and Gary White[‡]

[†]Department of Pharmaceutical Sciences, University of Oklahoma Health Science Center
Oklahoma City, OK

[‡]Department of Comparative Medicine University of Oklahoma Health Science Center Oklahoma
City, OK

Abstract

Dendritic cells (DCs) are the most potent antigen-presenting cells, but the ontogeny and functions of lung DCs are not known during prenatal period. Here, we isolated lung DC population from fetal (125–175dGA) and adult baboons. The cells were stained with fluorochrome-conjugated-HLA-DP, DQ, DR, CD1a, CD11c, CD14, CD40, CD80, CD86, CD209, CMKLR1, ILT7-specific antibodies, and staining was analyzed by Flow-cytometry. The phagocytic function was investigated by incubating the cells with fluorescent-labeled *Escherichia coli* bioparticles and analyzed by Flow-cytometry and fluorescence microscopy. The fetal baboon lung DCs expressed low levels of HLA-DP, DQ, DR, CD11c and CD86 as compared to adult baboon lung DCs and showed distinct DC morphology. The fetal lung DCs were also less capable of phagocytosing *E. coli* as compared to the adult lung DCs ($p < 0.05$). In conclusion, the fetal lung DCs are not only phenotypically immature, but also less efficient in phagocytosing *E. coli*.

Keywords

Dendritic cells; Innate immunity; Phenotype; Phagocytosis

Introduction

The preterm infants are very susceptible to respiratory infection during the first year of their life 1-4. The increased susceptibility of preterm infants to respiratory infections is associated with immature lung and poorly developed immune system. The developmental aspects of various immune components and their involvement in infection remain to be understood. Specifically, at the onset of infection, the antigen-presenting cells are the first type of immune cells that encounter the pathogens and define the downstream host defense mechanisms. Among various types of antigen-presenting cells, dendritic cells (DCs) have

Users may view, print, copy, and download text and data-mine the content in such documents, for the purposes of academic research, subject always to the full Conditions of use:http://www.nature.com/authors/editorial_policies/license.html#terms

^{*}Corresponding author Department of Pharmaceutical Sciences University of Oklahoma Health Science Center 1110 N. Stonewall Avenue, Oklahoma City, OK-73117 Ph:405–271–6593 (X47332) Fax: 405–271–7505 e-mail: Shanjana-Awasthi@ouhsc.edu.

Part of the present work was accepted for presentation at 2006 American Thoracic Society Meeting, San Francisco, CA.

been recognized as the most potent antigen-presenting cells 5-8. The DCs are present in both lymphoid and non-lymphoid organs of the body, and play a key role in mounting immune response against pathogens. The DCs are activated after coming in contact with pathogens, pathogen-derived ligands, foreign particles and endogenous stress signals 9. The activated DCs move to local lymph nodes where they stimulate naïve T cells, B cells or other immune cells, and regulate the stress-, antigen- or pathogen- specific adaptive immune response 10.

Although several studies have confirmed the immunomodulatory role of lung DCs against respiratory pathogens in adult humans and animal models 11-16, the ontogeny of lung DCs and immune functions remain unclear in preterm infants who are highly susceptible to respiratory infections. Thus, it is important to investigate the ontogeny, phenotypic characteristics and functions of pulmonary DCs during prenatal life.

A few studies on fetal rat and mouse lung DCs 11, 17, 18, mainly focus on histological examination of fetal lung tissues for cell-staining with MHC class II-antibody. The staining with antibodies against MHC class II or a single cell-surface marker is not helpful in identifying DCs, because DCs are identified based on the expression of a set of markers, for eg. MHC, T cell co-stimulatory molecules. As such, the pulmonary epithelial cells and macrophages also express MHC class II molecules on their cell surface 19. The expression of a combination of markers only determines the presence and type of DCs. Thus, for the phenotyping and functional studies, it is important to first isolate the lung DCs. One recent study was conducted on neonatal lamb model of RSV infection 12, in which the functions of isolated neonatal lung DCs were elucidated *in vitro*. However, there was no information on the phenotype and functions of lung DCs from fetal/preterm counterparts. From other smaller animal models (for example rat and mouse pups), it is very difficult to culture enough number of cells because of the smaller organ size. In this study, we investigated the phenotype and phagocytic ability of the isolated lung DCs of fetal and adult baboons. The larger size of lung in fetal baboons as compared to fetal mice, rats and other smaller animal models, allows the harvesting of sufficient number of cells for such an investigation. Moreover, because of ethical reasons, these studies are not possible in humans. Baboons are evolutionary close to humans, and their immune system is quite similar to the humans 20, 21.

Materials and Methods

Baboon lung tissues

The animal studies were approved by Institutional Animal Care and Use Committees, Environmental Health and Safety or Institutional Biosafety Committee of the University of Texas Health Science Center at San Antonio, TX (UTHSCSA) and University of Oklahoma Health Science Center, Oklahoma City, OK (OUHSC). Baboon (*Papio cynocephalus* and *P. anubis*) colonies are maintained at Southwest Foundation for Biomedical Research, San Antonio, TX and Baboon Resources, OUHSC, Oklahoma City, OK. At the time of necropsy, the whole fresh lung or a lobe of lung from fetal (delivered at 125, 140, 165 and 175 days of gestation; 125dGA, 140dGA, 165dGA, 175dGA, complete term = 185dGA) and adult baboons (age range 10–35 years, mean age 22.3 years) was collected in RPMI 1640 medium containing 2 mM glutamine, 1 mM N-2-Hydroxyethylpiperazine-N'-2-ethanesulfonic acid

(HEPES), 10 µg/ml gentamicin, 100 U/ml penicillin, 100 µg/ml streptomycin and 10% fetal bovine serum (low endotoxin <10EU/ml, FBS; Invitrogen, Carlsbad, CA). None of the animals recruited in this study showed any clinical sign of infection or lung pathology. Gross and microscopic examinations of all major viscera and the placenta revealed no signs of inflammation or infection.

Culture and isolation of lung DCs

Freshly collected lobe of the lung or whole lung samples were transported on ice in RPMI 1640 medium containing 2 mM glutamine, 1 mM HEPES, 10 µg/ml gentamicin, 100 U/ml penicillin, 100 µg/ml streptomycin and 10% FBS, cut and minced into small pieces using sterile scissors and forceps. We used only mild mechanical disruption to dissociate the tissue. Collagenase or trypsin enzyme treatment and osmotic shock were not used since these treatments may lead to loss of surface receptors and proteins 22-24. The finely-minced pieces of lung tissue were gently in-and-out pipetted using sterile transfer pipette and washed several times with culture medium. The single cell suspension was obtained after passing the minced lung tissue through nylon mesh. The fibrous material was washed several times with culture medium on top of the nylon mesh. The single cell suspension was seeded in tissue culture flask (Nalge-Nunc International Corp, Rochester, NY) at a density of $30\text{--}50 \times 10^6$ leukocytes/175 cm² flask in RPMI 1640 medium containing 2 mM glutamine, 1 mM HEPES, 10 µg/ml gentamicin, 100 U/ml penicillin, 100 µg/ml streptomycin and 10% FBS. The DCs were either harvested the same day within 30–60 min of collection (Day 0) or incubated overnight (16–18h; Day 1) at 37°C in 5% CO₂ atmosphere. The DC population was separated from RBCs, lymphocytes and granulocytes using OptiPrep cell-separation solution (density 1.32 g/ml, Accurate Chemicals, Westbury, NY) as described earlier 25. Briefly, $3\text{--}5 \times 10^6$ nonadherent cells were suspended in 3 ml of Hanks balanced salt solution (HBSS; Invitrogen, Carlsbad, CA) and 1 ml of OptiPrep solution (density 1.085 g/ml). The cell suspension was overlaid with 11.5% OptiPrep solution (density 1.065 g/ml) prepared in endotoxin-free diluent (0.88% NaCl, 1 mM EDTA, 0.5% bovine serum albumin and 10 mM HEPES) and centrifuged. The lung cells separated in different fractions (top, middle and bottom) of Optiprep density gradient solution with different density ranges were collected after centrifugation. The cell counts were taken, and viability was confirmed by trypan blue dye exclusion method. Since mature lung is assumed to have DC population 14, 26, which are isolated as low density cells on top of the Optiprep density gradient solution 27-29, first we confirmed the isolation of adult baboon lung DCs from other lung cells in the top fraction by immunophenotyping and microscopy. Similar method was then employed to characterize the fetal baboon lung DC population separated in the top fraction. The morphology and phenotype of lung cells collected from bottom and middle fractions of Optiprep density gradient were also characterized.

Light Microscopy

The isolated lung cells were air-dried on glass slides (Shandon, Pittsburgh, PA) and stained with Wright-Giemsa Diff-Quik stain (Dade Behring, Deerfield, IL). The cellular morphology of stained cells was then observed using Leica DM4000B or Nikon light microscope.

FACS analysis

The harvested baboon lung cells from top (with density <1.065 g/ml), bottom (with density > 1.085 g/ml) and middle (with density range 1.065–1.085 g/ml) fractions of density gradient were washed twice with Dulbecco's phosphate buffered saline (D-PBS) and suspended in D-PBS containing 1% FBS (10×10^6 cells per ml). The cells were incubated on ice for 30 min in dark with fluorochrome-conjugated antibodies (1 μ g per one million cells): fluorescein isothiocyanate (FITC), phycoerythrin (PE), allophycocyanin (APC) or biotin-conjugated, anti-human HLA-DP, DQ, DR (clone TU39), CD1a (clone SK9), CD40 (clone 5C3), CD86 (clone FUN-1), CD80 (clone BB1), CD14 (clone M5E2), CD11c (clone S-HCL-3), CMKLR1 (clone BZ332), CD209 or DC-SIGN (eb-H209) and ILT7 or CD85g (clone 17G10.2) antibodies (purchased from BD Biosciences, San Diego, CA or eBioscience, San Diego, CA) as described earlier 25. The cells were stained with cell-surface marker antibodies in the following combinations: (i) CD11c, CD14, (ii) CD1a, HLA-DP, DQ, DR, (iii) CD40, CD80, CD86, and (iv) CMKLR1, CD209, ILT7. To rule out the presence of lymphocytes, the harvested lung cells were also stained with FITC-conjugated anti-human CD2 (clone RPA 2.10, reactive with baboon T cells) and PE-conjugated anti-human CD20 (clone 2H7, reactive with baboon B cells) antibodies. Approximately 60–70% of the baboon monocytes and macrophages express CD14 as detected by flow cytometry (personal communication, Dr. Krishna K. Murthy, Department of Virology and Immunology, SFBR, San Antonio, TX); thus, we included CD14 specific antibody to identify monocytes or macrophages. The lung cells stained with biotinylated antibody were washed and further incubated with 1 μ g of streptavidin-APC conjugate (BD Biosciences, San Diego, CA) for 20 min. The appropriate isotype-matched control antibodies were used to determine the levels of background staining. Unstained cells were used as negative control to rule out autofluorescence. Fluorescence analysis was performed using a FACS Calibur flow cytometer (Becton-Dickinson Immunocytometry Systems, San Jose, CA). The histogram and dot plot data were collected and analyzed using CellQuest V3.1 (Becton-Dickinson Immunocytometry Systems, San Jose, CA), winMDI 2.8 (Joseph Trotter, The Scripps Research Institute, San Diego, CA) and Summit v 4.3 (Dako Colorado Inc, Fort Collins, CO) software programs. We gated the positive cells in the histogram charts and obtained mean fluorescent intensity (MFI) values.

Phagocytosis Assay

The phagocytic ability of DCs obtained from top fraction of the density gradient was studied using heat-killed, FITC-labeled, 0.2–2 μ m size, *E.coli* K12 bioparticles (Molecular Probes, Eugene, OR) 30. First, the bioparticles were incubated with 0.9% NaCl solution supplemented with 1 mM CaCl_2 , 1 mM MgCl_2 and 25% pooled healthy adult baboon sera for 30 min at 37°C in a shaking water bath. The opsonized bioparticles were washed twice, suspended in HEPES buffer containing 1 mM CaCl_2 and 1 mM MgCl_2 and sonicated (Braun Labsonic 2000 sonicator) for 3 cycles of 10 s each just before use. The isolated cells (5×10^6) were suspended in 1 mM HEPES buffer containing 1 mM CaCl_2 and 1 mM MgCl_2 and incubated at 37°C in a shaking water bath with serum-opsonized *E.coli* K12 bioparticles (1 cell: 10 *E.coli* K12 bioparticles). Another set of tubes was incubated on ice to serve as negative controls. To stop phagocytosis, incubation mixtures were withdrawn from water

bath and stored on ice. An equal volume of trypan blue solution (250 µg/ml diluted in 0.1 M citrate buffer, pH 4.0) was added to the tubes to quench the green fluorescence of extracellular bacteria attached on the cell surface. The quenching with trypan blue provides red fluorescence that can be detected by flow-cytometry. After 1 min incubation in ice, the samples were subjected to flow cytometry using a FACS Calibur flow cytometer at FACS Core Facility, UTHSCSA, San Antonio, TX or at FACS and Imaging Core Facility, OUHSC, Oklahoma City, OK. The cells were illuminated using 15 milliwatts of 488 nm argon ion laser light. FITC and red fluorescence were collected through a 530/30 nm (FL-1) and 670 nm (FL-3) band pass filters, respectively. The data were collected and analyzed using CellQuest V3.1 or winMDI2.8 software program.

Different stages of phagocytosis and % phagocytosis were further confirmed by fluorescence microscopy. After the incubation of cells with FITC-labeled *E.coli* bioparticles, the cells were stained with 1 µg/ml Hoechst 33342 dye (Invitrogen-Molecular Probes, CA). After staining for 1h at room temperature, the cells were fixed and observed under Leica 4000B fluorescence microscope for green (FITC) and blue (Hoechst 33342) fluorescence. Number of cells with ingested green fluorescent bioparticles was taken into account.

Statistical Analysis

The results were analyzed by Student's t-test for statistical significance using Prism software (Graphpad, San Diego, CA). $p < 0.05$ was considered significant.

Results

Morphologic characteristics of fetal and baboon lung cells with variable density separated on Optiprep density gradient

After density gradient separation, we collected lung cells from three distinct fractions: one at the bottom (density > 1.085 g/ml), second in the middle (density 1.065–1.085 g/ml) and third on the top (density < 1.065 g/ml). The lung cells with heavier density (> 1.085 g/ml) settled at the bottom. Morphologically, these cells appeared to be epithelial cells, macrophages and red blood cells. The cells in the middle fraction showed morphology similar to lymphocytes. In top fraction, the floating lung cells of adult baboon appeared as mature DCs. In contrast, the fetal baboon lung cells in top fraction were round, had vacuolar cytoplasm and did not possess the dendrites (Figure 1). We did not detect mature lung DCs in any of the fetal lung cell population obtained from top, bottom or middle fractions of density gradient. The fetal baboon lung cells collected from top of the density gradient were unique to fetal baboons, and were not identified in adult baboon. The morphologic features of lung cells were maintained, whether cells were harvested on day 0 or day 1, after 16–18h of culture (Figure 1).

Yield of fetal and adult baboon lung cells

Most of the cells (90–95%) settled in the bottom fraction after density gradient separation. Only 3–7% and 0.2–1% of the total lung cells were isolated in the middle and top fractions, respectively (Table 1). The yield of adult and fetal baboon lung cells isolated in the top fraction, varied from 0.1×10^6 – 1.3×10^6 per gram lung tissue. Approximately, 0.1 – 0.7×10^6 ,

$0.5\text{--}1.3\times 10^6$ and about $0.5\text{--}1\times 10^6$ cells were harvested in the top fraction per gram lung tissue of 125–140dGA, 165–175dGA and adult baboons, respectively.

Immunophenotype of lung cells isolated in middle and bottom fractions after density gradient centrifugation

For immunophenotyping of lung cells in different fractions, the flow-cytometry was performed. Flow-cytometry analysis of antibody-stained lung cells in bottom fraction show that both adult and fetal baboon cells were negative for CD2, CD20, CD1a, CD11c, DC-SIGN (CD209), CMKLR1, IL-T7 (CD85g), CD40 and CD86. Only very few adult baboon lung cells were positive for HLA-DP,DQ,DR (upto 5%) as compared to negligible staining by fetal baboon lung cells. Morphologically, most of the cells showed features similar to red blood cells, macrophages and large epithelial cells.

In the middle fraction, however, 80% of the adult baboon lung cells with small forward and side scatter were positive for CD2 (lymphocyte cell marker). In contrast, only 11–12% of fetal baboon lung cells isolated in the middle fraction were positive for CD2 marker. The morphology of these cells was similar to the normal typical lymphocytes: condensed nucleus and scant cytoplasm.

The immunophenotype of the lung cells obtained from bottom or middle fractions of density gradient was same on day 0 and day 1 of harvesting.

Immunophenotype of lung cells separated in the top fraction

The adult and fetal baboon lung cells separated in the top fraction were always negative for CD2 (T cell marker), CD20 (B cell marker) and CD14 (monocyte-macrophage marker) (Figure 2). These cells were also negative for plasmacytoid DC markers: CMKLR1 31, CD209 32 and ILT7 33. The FACS analysis of cells with large forward and side scatter shows that as compared to adult baboon lung DCs (~40% positive for HLA-DP,DQ,DR), only 5.5% fetal lung cells were positive for HLA-DP,DQ, DR marker (Table 2). Thirty-one and 15% of adult baboon lung DCs were positive for CD86 and CD11c, respectively, as compared to 10.8% and 5.8% of fetal baboon lung cells separated in the top fraction (Table 2). Only 9% of adult baboon lung DCs expressed CD80 as compared to 18% of fetal baboon lung cells (Table 2). Both fetal and adult baboon lung cells with small forward and side scatter stained with low MFI (negligible staining) for these markers.

The MFI of HLA-DP, DQ, DR (MHC II), CD1a, CD14, CD11c, CD40, CD80 and CD86 markers was further analyzed by plotting the FACS histograms (Figure 3). The results suggest that the MFI values for HLA-DP,DQ,DR, CD11c and CD86 were higher for adult baboon lung DCs as compared to fetal baboon lung cells obtained from the top fraction. However, the MFI value for CD80 was low in lung DCs of adult baboons as compared to the fetal baboon lung cells. The immunophenotype of fetal and adult baboon lung cells harvested on day 0 was not different from those harvested on day 1 after 16–18h of culture (data not shown).

Based on the morphologic, immunophenotypic and isolation characteristics, it is clear that the adult baboon lung DCs are separated as low-density cells in the top fraction of Optiprep

density gradient. Previous literature reports in different adult animal models, also support this observation 15, 27-29. A significant number of fetal baboon lung cells with low-density are also isolated in the same top fraction of Optiprep density gradient. These fetal baboon lung cells are morphologically different from mature adult baboon lung DCs, and show unique morphologic and phenotypic characteristics distinct from macrophages, monocytes, lymphocytes, epithelial cells and other kind of immune cells. Fetal baboon lung cells separated in the top fraction stained low for the typical DC-markers and morphologically appeared similar to the immature DCs without dendrites on their cell surface. Based on these results, we believe that these fetal baboon lung cells probably represent the DC-precursor cells that may transform into mature DCs after birth and during adulthood.

Phagocytosis of heat-killed, FITC-labeled *E.coli* K12 bioparticles by DCs

After the isolation of lung DCs or DC-precursor cells from adult and fetal baboons, we confirmed their viability and phagocytic function. Approximately 90–95% cells were viable. Phagocytic capacity of lung DCs or DC-precursor cells was determined by flow cytometric dot-plot analysis (Figure 4). The phagocytosis assay was performed using serum-opsonized, fluorescent-labeled, heat-killed *E. coli* bioparticles. The x-axis represents the green fluorescence (FL-1 channel) and y-axis represents the red fluorescence (FL-3 channel; Figure 4). When extracellular FITC-labeled bacteria are present on the surface of the cells, trypan blue quenches the green fluorescence of FITC and cells fluoresce red. The cells with surface-adherent bacteria (red fluorescence) are shown in upper quadrants. The cells with phagocytosed FITC-labeled bacteria (green fluorescence) are shown in right quadrants. When the reaction was performed on ice (negative control), the lung DCs were found distributed in only two left quadrants without any phagocytosed particles (Figure 4). In phagocytosis assay tubes (performed at 37°C), cell populations were identified distributed in all four quadrants (Figure 4). Lower left quadrant contains nonfluorescent events corresponding to cells without any associated particles (no interaction), upper left quadrant contains cells with only membrane-bound *E.coli* bacteria (adherence), upper right quadrant contains cells with both internalized and surface-associated *E.coli* bioparticles (adherence and ingestion) and lower right quadrant corresponds to green fluorescent events of cells with ingested *E.coli* bioparticles (phagocytosis). The percent phagocytosis of *E. coli* bioparticles was further confirmed by fluorescence microscopy. Representative photomicrograph is shown in Figure 4. There was significant difference in phagocytic ability of fetal baboon lung DC-precursor cells from that of adult baboon lung DCs ($p < 0.05$, Table 3, Figure 4). The fetal baboon lung DC-precursor cells were 3 (175dGA), 10 (165dGA) and 150 (125–140dGA)-folds less capable of phagocytosing *E.coli* bioparticles as compared to the adult baboon lung DCs (Table 3).

Discussion

Very few published studies are available in the literature that focus on the functions of *in vitro* neonatal- macrophages and cord blood- or blood monocyte-derived DCs 34-39. Results of our earlier study on fetal baboon bone marrow-derived DCs provide evidence that the DC functions (phagocytosis and cytokine secretion) are impaired during prenatal fetal life in baboons 25. In our previous study, we had cultured DCs using bone marrow samples of

fetal, close-to-term and adult baboons in presence of GM-CSF and IL-4 25. The fetal baboon bone marrow-derived DCs were morphologically and phenotypically similar to adult baboon bone marrow-derived DCs. Irrespective of gestation age of fetal baboons or age of the adult baboon, the cell surface expression of all the DC markers was found to increase as the duration of incubation increased in culture medium containing GM-CSF and IL-4 25. The phenotypes of *in vitro* bone marrow-derived DCs are different from lung DCs as evident from these studies. Thus, it is difficult to extend the results from *in vitro*-derived DCs to resident DCs in various tissues. To study the role of DCs in pulmonary innate immunity, it is important to conduct focused study on resident lung DCs. Such studies with fetal lung DCs are very difficult to perform because the lung tissue of fetal rodents is very small to obtain sufficient number of cells. Moreover, these investigations cannot be conducted in human fetuses due to ethical reasons. Because the immunology, anatomy and physiology of non-human primate are very similar to humans and preterm baboon model mimics the clinical situation of preterm infants 40, studies in preterm baboons are highly relevant.

The lung DCs make only 1% of total lung cell population 41-43, therefore it is very difficult to isolate these cells in sufficient quantity for functional studies. In the past, lung DCs have been cultured using collagenase and trypsin enzymatic treatment, or in combination with positive selection using antibody (for example CD11c)-bound columns or Percoll density gradient 12, 15, 44, 45. There are reasons to believe that the collagenase, trypsin and osmotic shock treatment may disrupt the cell-surface receptors 22-24. Since there is no lung DC-specific marker known, and antibody-based positive selection method for isolating DCs has its own limitations, it is difficult to interpret the immunophenotype of the natural resident lung DCs from the published studies. We simplified the isolation procedure in this study and utilized only slow mechanical disruption and gentle processing. We believe that the DCs harvested using this method closely represent the unmodified, natural primary DC population present *in vivo* in lung. However, the yield of lung DCs from adult baboons was found much lower (1×10^6 cells/g wet lung) compared to the yield of lung DCs from adult humans as published earlier 15. This discrepancy could be due to the differences in methods for isolation and collection. In the study by Masten et al 15, the lung DCs were collected from the density range (1.030–1.075 g/ml) of Percoll-gradient which may have led to harvesting of increased number of cells including non-DCs 15. In this study, however, we collected the lung DCs only from the top of 11.5% Optiprep solution (density < 1.065 g/ml; Accurate Chemicals, NY). Earlier, we have been successful in using Optiprep density gradient solution to harvest *in vitro* bone marrow-derived DCs of baboons and obtained good yield 25. Previously, the Optiprep density gradient solution has also been used successfully for purification of DCs from liver 46, 47, lung 27-29, lymph, lymph node 48, spleen 49, blood 50 and other tissues 51 by other investigators.

This is the first study when isolation, phenotypic and functional characteristics of lung DCs or DC-precursor cells have been studied to compare adult and fetal DC-population. Based on phenotypic characteristics, such as absence of CD2, CD20, CD14, positive (but low) staining with HLA-DP,DQ,DR, CD11c, CD80 and CD86 and similar cellular density, we identify that these fetal baboon lung cells probably represent the DC-precursor cells. The

fetal baboon lung DC-precursor cells are more vacuolar and do not present the tentacles on their cell surface (characteristic of mature DCs). As compared to the fetal baboon lung DCs, the adult baboon lung DCs exhibited the long dendrites (Figure 1). Since, the fetal baboons are not exposed to external stimuli (dust, pathogens etc), that are inhaled continually in lung after birth, we would expect the DCs or DC precursor cells to be present in immature form in lungs of fetuses or preterm animals. It is possible that same DC-precursor cells would develop into mature DCs during the process of attaining adulthood. A recent study suggests that the lung DCs of both neonatal and adult sheep are phenotypically and functionally similar 45. It is conceivable that preterm/fetal lung DCs are immature and immunodeficient as compared to the lung DCs from full-term neonates as well.

The number of positive cells and MFI values for CD11c, HLA-DP, DQ, DR (MHC II) and CD86 markers were found increased in adult baboon lung DCs. On the other hand, the expression of CD80 was increased on cell surface of fetal baboon lung DC-precursor cells as compared to the adult baboon lung DCs (Figure 3, Table 2). The expression pattern of CD40, CD80 and CD86 by adult baboon lung DCs is comparable with previously published results on adult human lung DCs 44. With the help of different pathogen-pattern recognition receptors (PPRRs) including Toll-like receptors, the antigen-presenting cells including DCs are able to recognize and phagocytose the pathogens 52. The phagocytosis of pathogens or foreign particles is an important functional characteristic of DCs 53. Thus, we studied the phagocytic ability of lung DCs by incubating them with fluorescent-labeled *E. coli* bioparticles as described earlier 25. We found that similar to the bone marrow-derived DCs 25, the primary resident lung DC-precursor cells of fetal baboons are less capable of phagocytosing *E. coli* bioparticles (Figure 4, Table 3).

To our knowledge, this is the first report focused on studying the phenotypic and phagocytic ability of isolated fetal lung DC-precursor cells. Most of the studies available in literature are focused on the localization of lung DCs or DC-precursor cells in fetal lung tissues of rodents and humans by immunohistology after staining with—Ia (MHC class II, HLA-DR) and DC-SIGN (C-type lectin expressed on cell-surface of plasmacytoid DCs) 11, 17, 18, 32, 54, 55. Results from these studies suggest that Ia+ cells are present even at day 17 of gestation in fetal rats (77% of full term, term period ~ 22 days), but these cells were only 40–60% effective in stimulating T cell proliferation as compared to adult lung Ia+ cells 17. The Ia+ cells were also present at 12 weeks of gestation in human fetal lung, kidney, heart and pancreas (31% of full term, term period ~ 38 weeks) 54. In an ensuing study by Soilleux et al, a plasmacytoid DC marker: DC-SIGN or CD209 was used to characterize the density and distribution of DCs in fetal and adult human lung tissues by immunohistology 32; the fetal lung tissue stained positive for DC-SIGN (CD209) and cells looked similar to non-dendritic macrophages, positive for CD14. In contrast, in the present study, the isolated fetal baboon lung DC-precursor cells or adult baboon lung DCs did not stain with CD14 (Figure 2) or CD209-specific antibody (data not shown). The isolated lung cells also did not stain with any of the other plasmacytoid DC-markers (CMKLR1 and ILT7)-specific antibody. These results suggest that the isolated fetal and adult baboon lung DC populations are mainly of myeloid type.

In conclusion, we report that the fetal lung DCs are immature and functionally deficient in responding to gram-negative bacterial stimuli. We believe that these results in non-human primate model will be translatable to humans. Future studies with isolated fetal baboon lung DC population would be very useful in understanding the immunostimulatory functions and their role in early childhood diseases.

Acknowledgement

Authors thank Charles A. Thomas, Institutional FACS Core Facility, University of Texas Health Science Center at San Antonio (UTHSCSA) and Jim Henthorn, FACS and Imaging Core Facility, University of Oklahoma Health Science Center (OUHSC) for their assistance in FACS analysis. Fresh lung tissue samples of fetal animals were obtained from Baboon Resources (Director: Dr. Gary white, OUHSC), BPD Baboon Resource Center (Director: Dr. Jacqueline J. Coalson, UTHSCSA) and Center for Pregnancy and Newborn Research (Director: Dr. Peter W. Nathanielsz, UTHSCSA). The lung tissues of adult baboons were obtained from Southwest Foundation of Biomedical Research, San Antonio and Baboon Resources, OUHSC. Authors acknowledge technical help from Jodie Cropper and Kevin Brown.

Source of Support: This work was supported by research grants from American Lung Association and Presbyterian Health Foundation. The project described was partially supported by Grant Number P40RR012317 (at OUHSC) from the National Center for Research Resources.

Abbreviations

APC	Allophycocyanin
DC(s)	Dendritic cell(s)
dGA	days of gestation age
D-PBS	Dulbecco's phosphate buffered saline
FACS	Flow activated cell sorting
FBS	Fetal bovine serum
FITC	Fluorescein isothiocyanate
HBSS	Hanks balanced salt solution
HEPES	N-2-Hydroxyethylpiperazine-N'-2-ethanesulfonic acid
MFI	Mean Fluorescent Intensity
PE	Phycoerythrin
SEM	standard error of measurement

References

1. de Mello RR, Dutra MV, Lopes JM. [Respiratory morbidity in the first year of life of preterm infants discharged from a neonatal intensive care unit]. *J Pediatr (Rio J)*. 2004; 80:503–10. [PubMed: 15622428]
2. de Mello RR, Dutra MV, Ramos JR, Daltro P, Boechat M, Lopes JM. Neonatal risk factors for respiratory morbidity during the first year of life among premature infants. *Sao Paulo Med J*. 2006; 124:77–84. [PubMed: 16878190]
3. Blaymore Bier JA, Oliver T, Ferguson A, Vohr BR. Human milk reduces outpatient upper respiratory symptoms in premature infants during their first year of life. *J Perinatol*. 2002; 22:354–9. [PubMed: 12082468]

4. Greenough A, Maconochie I, Yuksel B. Recurrent respiratory symptoms in the first year of life following preterm delivery. *J Perinat Med.* 1990; 18:489–94. [PubMed: 2097342]
5. Fajardo-Moser M, Berzel S, Moll H. Mechanisms of dendritic cell-based vaccination against infection. *Int J Med Microbiol.* 2008; 298:11–20. [PubMed: 17719274]
6. Ohteki T. The dynamics of dendritic cell: mediated innate immune regulation. *Allergol Int.* 2007; 56:209–14. [PubMed: 17646738]
7. Sabatte J, Maggini J, Nahmod K, Amaral MM, Martinez D, Salamone G, et al. Interplay of pathogens, cytokines and other stress signals in the regulation of dendritic cell function. *Cytokine Growth Factor Rev.* 2007; 18:5–17. [PubMed: 17321783]
8. van Vliet SJ, Dunnen J, Gringhuis SI, Geijtenbeek TB, van Kooyk Y. Innate signaling and regulation of Dendritic cell immunity. *Curr Opin Immunol.* 2007; 19:435–40. [PubMed: 17629469]
9. Kapsenberg ML. Dendritic-cell control of pathogen-driven T-cell polarization. *Nat Rev Immunol.* 2003; 3:984–93. [PubMed: 14647480]
10. Steinman RM. Some interfaces of dendritic cell biology. *Apmis.* 2003; 111:675–97. [PubMed: 12974772]
11. Banks EM, Kyriakidou M, Little S, Hamblin AS. Epithelial lymphocyte and macrophage distribution in the adult and fetal equine lung. *J Comp Pathol.* 1999; 120:1–13. [PubMed: 10098012]
12. Fach SJ, Meyerholz DK, Gallup JM, Ackermann MR, Lehmkuhl HD, Sacco RE. Neonatal ovine pulmonary dendritic cells support bovine respiratory syncytial virus replication with enhanced interleukin (IL)-4 And IL-10 gene transcripts. *Viral Immunol.* 2007; 20:119–30. [PubMed: 17425426]
13. Holt PG, Nelson DJ, McWilliam AS. Population dynamics and functions of respiratory tract dendritic cells in the rat. *Adv Exp Med Biol.* 1995; 378:177–81. [PubMed: 8526049]
14. Lommatzsch M, Bratke K, Bier A, Julius P, Kuepper M, Luttmann W, et al. Airway dendritic cell phenotypes in inflammatory diseases of the human lung. *Eur Respir J.* 2007; 30:878–86. [PubMed: 17626112]
15. Masten BJ, Olson GK, Tarleton CA, Rund C, Schuyler M, Mehran R, et al. Characterization of myeloid and plasmacytoid dendritic cells in human lung. *J Immunol.* 2006; 177:7784–93. [PubMed: 17114449]
16. Webb TJ, Sumpter TL, Thiele AT, Swanson KA, Wilkes DS. The phenotype and function of lung dendritic cells. *Crit Rev Immunol.* 2005; 25:465–91. [PubMed: 16390323]
17. McCarthy KM, Gong JL, Telford JR, Schneeberger EE. Ontogeny of Ia⁺ accessory cells in fetal and newborn rat lung. *Am J Respir Cell Mol Biol.* 1992; 6:349–56. [PubMed: 1540399]
18. Nelson DJ, McMenamin C, McWilliam AS, Brenan M, Holt PG. Development of the airway intraepithelial dendritic cell network in the rat from class II major histocompatibility (Ia)-negative precursors: differential regulation of Ia expression at different levels of the respiratory tract. *J Exp Med.* 1994; 179:203–12. [PubMed: 8270865]
19. Cunningham AC, Zhang JG, Moy JV, Ali S, Kirby JA. A comparison of the antigen-presenting capabilities of class II MHC-expressing human lung epithelial and endothelial cells. *Immunology.* 1997; 91:458–63. [PubMed: 9301537]
20. Patterson JL, Carrion R Jr. Demand for nonhuman primate resources in the age of biodefense. *Ilar J.* 2005; 46:15–22. [PubMed: 15644560]
21. Sibal LR, Samson KJ. Nonhuman primates: a critical role in current disease research. *Ilar J.* 2001; 42:74–84. [PubMed: 11406709]
22. Dezutter-Dambuyant C, Schmitt D, Staquet MJ, Boumsell L, Thivolet J. Cleavage of Langerhans cell surface CD1a molecule by trypsin. *Res Immunol.* 1989; 140:377–90. [PubMed: 2476841]
23. Nagaeva O, Bondestam K, Olofsson J, Damber MG, Mincheva-Nilsson L. An optimized technique for separation of human decidual leukocytes for cellular and molecular analyses. *Am J Reprod Immunol.* 2002; 47:203–12. [PubMed: 12069387]
24. White HD, Prabhala RH, Humphrey SL, Crassi KM, Richardson JM, Wira CR. A method for the dispersal and characterization of leukocytes from the human female reproductive tract. *Am J Reprod Immunol.* 2000; 44:96–103. [PubMed: 10994637]

25. Awasthi S, Cropper J. Immunophenotype and functions of fetal baboon bone-marrow derived dendritic cells. *Cell Immunol.* 2006; 240:31–40. [PubMed: 16842767]
26. de Heer HJ, Hammad H, Kool M, Lambrecht BN. Dendritic cell subsets and immune regulation in the lung. *Semin Immunol.* 2005; 17:295–303. [PubMed: 15967679]
27. Hayashi T, Beck L, Rossetto C, Gong X, Takikawa O, Takabayashi K, et al. Inhibition of experimental asthma by indoleamine 2,3-dioxygenase. *J Clin Invest.* 2004; 114:270–9. [PubMed: 15254594]
28. Majlessi L, Brodin P, Brosch R, Rojas MJ, Khun H, Huerre M, et al. Influence of ESAT-6 secretion system 1 (RD1) of *Mycobacterium tuberculosis* on the interaction between mycobacteria and the host immune system. *J Immunol.* 2005; 174:3570–9. [PubMed: 15749894]
29. Okunishi K, Dohi M, Nakagome K, Tanaka R, Mizuno S, Matsumoto K, et al. A novel role of hepatocyte growth factor as an immune regulator through suppressing dendritic cell function. *J Immunol.* 2005; 175:4745–53. [PubMed: 16177122]
30. Busetto S, Trevisan E, Patriarca P, Menegazzi R. A single-step, sensitive flow cytometric assay for the simultaneous assessment of membrane-bound and ingested *Candida albicans* in phagocytosing neutrophils. *Cytometry A.* 2004; 58A:201–6. [PubMed: 15057974]
31. Zabel BA, Silverio AM, Butcher EC. Chemokine-like receptor 1 expression and chemerin-directed chemotaxis distinguish plasmacytoid from myeloid dendritic cells in human blood. *J Immunol.* 2005; 174:244–51. [PubMed: 15611246]
32. Soilleux EJ, Morris LS, Leslie G, Chehimi J, Luo Q, Levroney E, et al. Constitutive and induced expression of DC-SIGN on dendritic cell and macrophage subpopulations in situ and in vitro. *J Leukoc Biol.* 2002; 71:445–57. [PubMed: 11867682]
33. Cho M, Ishida K, Chen J, Ohkawa J, Chen W, Namiki S, et al. SAGE library screening reveals ILT7 as a specific plasmacytoid dendritic cell marker that regulates type I IFN production. *Int Immunol.* 2008; 20:155–64. [PubMed: 18048391]
34. Chelvarajan RL, Collins SM, Doubinskaia IE, Goes S, Van Willigen J, Flanagan D, et al. Defective macrophage function in neonates and its impact on unresponsiveness of neonates to polysaccharide antigens. *J Leukoc Biol.* 2004; 75:982–94. [PubMed: 14982942]
35. Goriely S, Vincart B, Stordeur P, Vekemans J, Willems F, Goldman M, et al. Deficient IL-12(p35) gene expression by dendritic cells derived from neonatal monocytes. *J Immunol.* 2001; 166:2141–6. [PubMed: 11160266]
36. Liu E, Tu W, Law HK, Lau YL. Decreased yield, phenotypic expression and function of immature monocyte-derived dendritic cells in cord blood. *Br J Haematol.* 2001; 113:240–6. [PubMed: 11328307]
37. Petty RE, Hunt DW. Neonatal dendritic cells. *Vaccine.* 1998; 16:1378–82. [PubMed: 9711775]
38. Upham JW, Lee PT, Holt BJ, Heaton T, Prescott SL, Sharp MJ, et al. Development of interleukin-12-producing capacity throughout childhood. *Infect Immun.* 2002; 70:6583–8. [PubMed: 12438328]
39. Salio M, Dulphy N, Renneson J, Herbert M, McMichael A, Marchant A, et al. Efficient priming of antigen-specific cytotoxic T lymphocytes by human cord blood dendritic cells. *Int Immunol.* 2003; 15:1265–73. [PubMed: 13679395]
40. Coalson JJ, Winter VT, Siler-Khodr T, Yoder BA. Neonatal chronic lung disease in extremely immature baboons. *Am J Respir Crit Care Med.* 1999; 160:1333–46. [PubMed: 10508826]
41. Masten, BJ.; Lipscomb, MF. Methods to isolate and study lung dendritic cells.. In: Lipscomb, MF.; Russell, SW., editors. *Lung Macrophages and Dendritic Cells in Health and Disease.* Marcel Dekker Inc.; New York: 1997. p. 223-238.
42. McWilliam AS, Holt PG. Immunobiology of dendritic cells in the respiratory tract: steady-state and inflammatory sentinels? *Toxicol Lett.* 1998; 102-103:323–9. [PubMed: 10022273]
43. McWilliam AS, Napoli S, Marsh AM, Pemper FL, Nelson DJ, Pimm CL, et al. Dendritic cells are recruited into the airway epithelium during the inflammatory response to a broad spectrum of stimuli. *J Exp Med.* 1996; 184:2429–32. [PubMed: 8976199]
44. Cochand L, Isler P, Songeon F, Nicod LP. Human lung dendritic cells have an immature phenotype with efficient mannose receptors. *Am J Respir Cell Mol Biol.* 1999; 21:547–54. [PubMed: 10536111]

45. Fach SJ, Brockmeier SL, Hobbs LA, Lehmkühl HD, Sacco RE. Pulmonary dendritic cells isolated from neonatal and adult ovine lung tissue. *Vet Immunol Immunopathol.* 2006; 112:171–82. [PubMed: 16621027]
46. Cremer I, Dieu-Nosjean MC, Marechal S, Dezutter-Dambuyant C, Goddard S, Adams D, et al. Long-lived immature dendritic cells mediated by TRANCE-RANK interaction. *Blood.* 2002; 100:3646–55. [PubMed: 12393586]
47. Goddard S, Youster J, Morgan E, Adams DH. Interleukin-10 secretion differentiates dendritic cells from human liver and skin. *Am J Pathol.* 2004; 164:511–9. [PubMed: 14742257]
48. Schwartz-Cornil I, Epardaud M, Bonneau M. Cervical duct cannulation in sheep for collection of afferent lymph dendritic cells from head tissues. *Nat Protoc.* 2006; 1:874–9. [PubMed: 17406320]
49. Zarnani AH, Moazzeni SM, Shokri F, Salehnia M, Dokouhaki P, Shojaeian J, et al. The efficient isolation of murine splenic dendritic cells and their cytochemical features. *Histochem Cell Biol.* 2006; 126:275–82. [PubMed: 16607536]
50. Akiyama Y, Tanosaki R, Inoue N, Shimada M, Hotate Y, Yamamoto A, et al. Clinical response in Japanese metastatic melanoma patients treated with peptide cocktail-pulsed dendritic cells. *J Transl Med.* 2005; 3:4. [PubMed: 15676080]
51. De Bernardis F, Lucciarini R, Boccanera M, Amantini C, Arancia S, Morrone S, et al. Phenotypic and functional characterization of vaginal dendritic cells in a rat model of *Candida albicans* vaginitis. *Infect Immun.* 2006; 74:4282–94. [PubMed: 16790803]
52. Akira S, Takeda K. Toll-like receptor signalling. *Nat Rev Immunol.* 2004; 4:499–511. [PubMed: 15229469]
53. Guermonprez P, Valladeau J, Zitvogel L, Thery C, Amigorena S. Antigen presentation and T cell stimulation by dendritic cells. *Annu Rev Immunol.* 2002; 20:621–67. [PubMed: 11861614]
54. Hofman FM, Danilovs JA, Taylor CR. HLA-DR (Ia)-positive dendritic-like cells in human fetal nonlymphoid tissues. *Transplantation.* 1984; 37:590–4. [PubMed: 6587648]
55. Holt PG. Dendritic cell ontogeny as an aetiological factor in respiratory tract diseases in early life. *Thorax.* 2001; 56:419–20. [PubMed: 11359953]

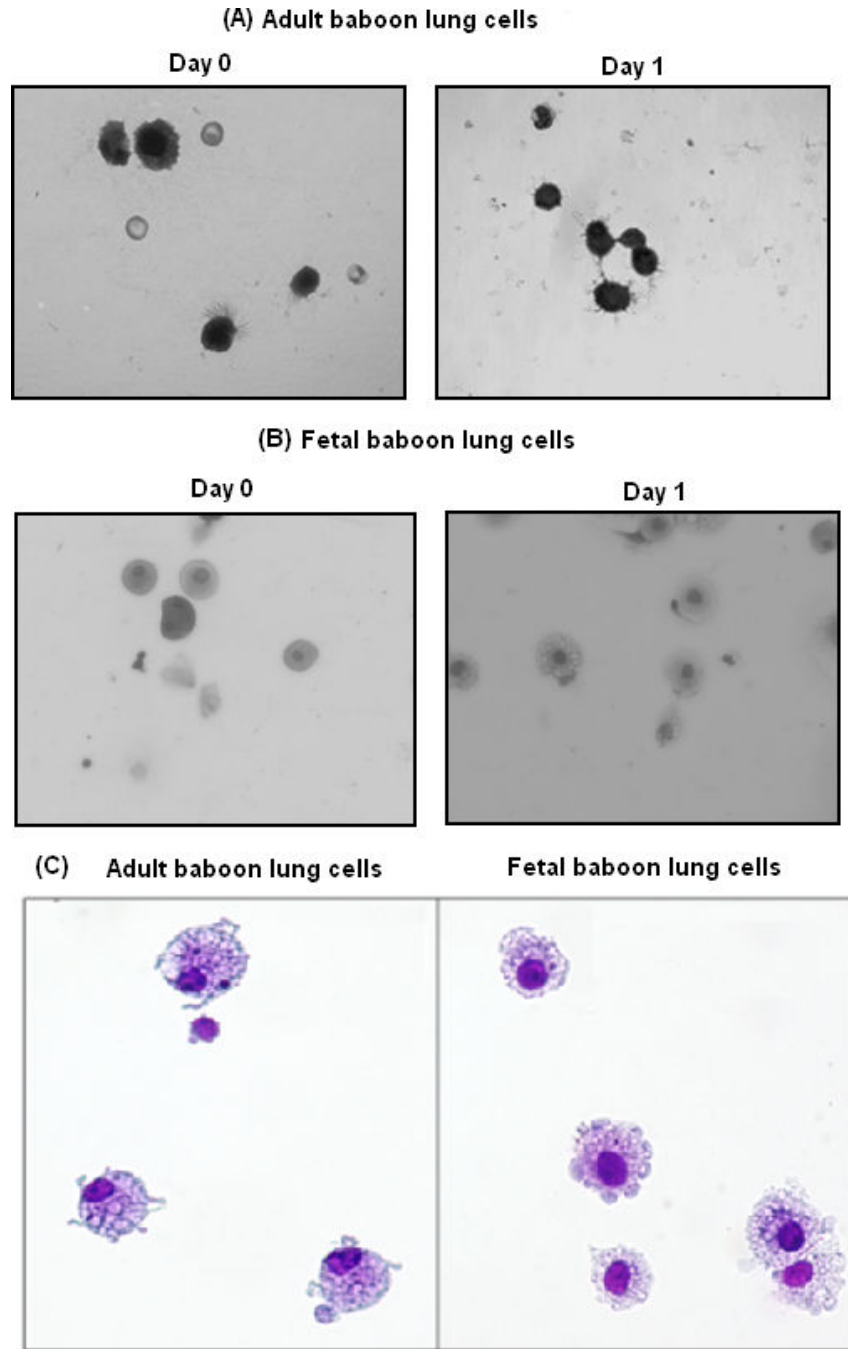


Figure 1. Wright-Giemsa stained, air-dried preparation of baboon lung cells obtained from the top fraction (density <math><1.065\text{ g/ml}</math>) after density gradient separation. Lung cells of adult (A) and fetal baboons (B) were harvested immediately after collection (Day 0) or after 16–18h of culture (Day 1). Lung cells were collected, air-dried on glass slides and stained with Wright-Giemsa Diff-Quik stain. The stained cells were observed under light microscope and photomicrographs were taken using 100X objective lens. (C) Representative photomicrographs (at higher magnification) of Wright-Giemsa stained adult and fetal

baboon lung cells collected from the top fraction. The pictures were acquired and assembled using Spot (Diagnostics Instruments Inc., MI) or Nikon ACT-1 ver-2 software program.

Author Manuscript

Author Manuscript

Author Manuscript

Author Manuscript

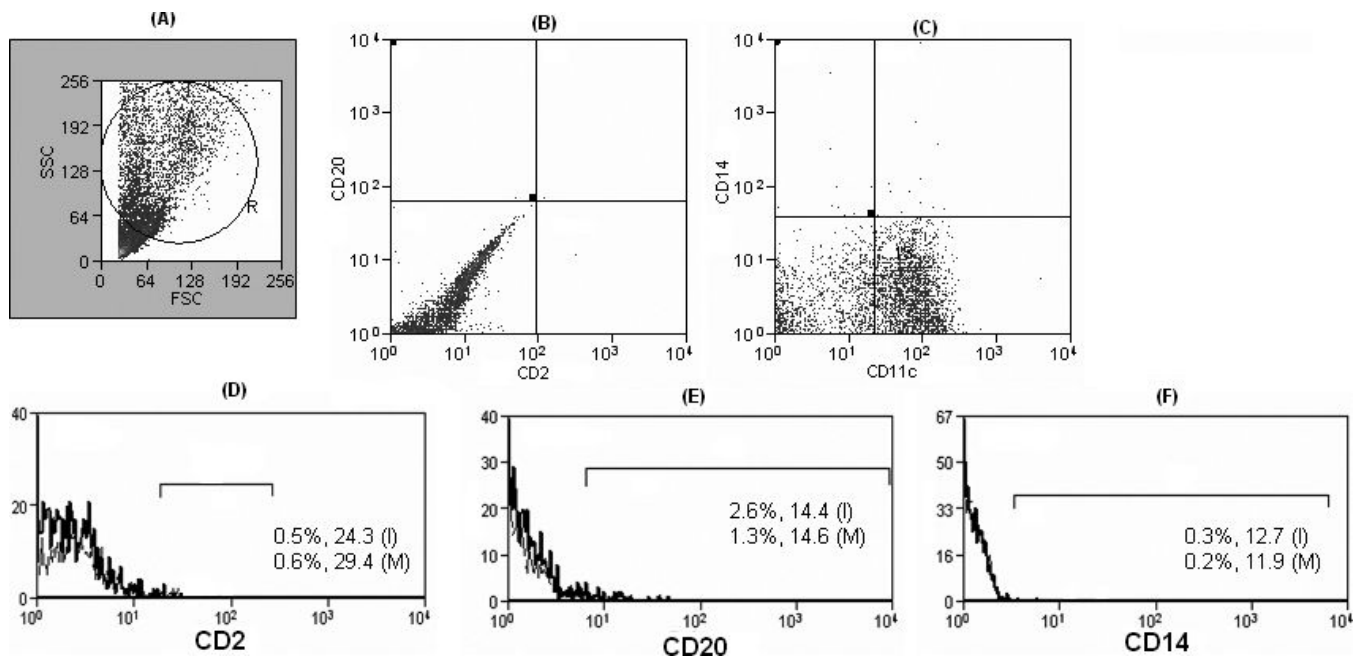
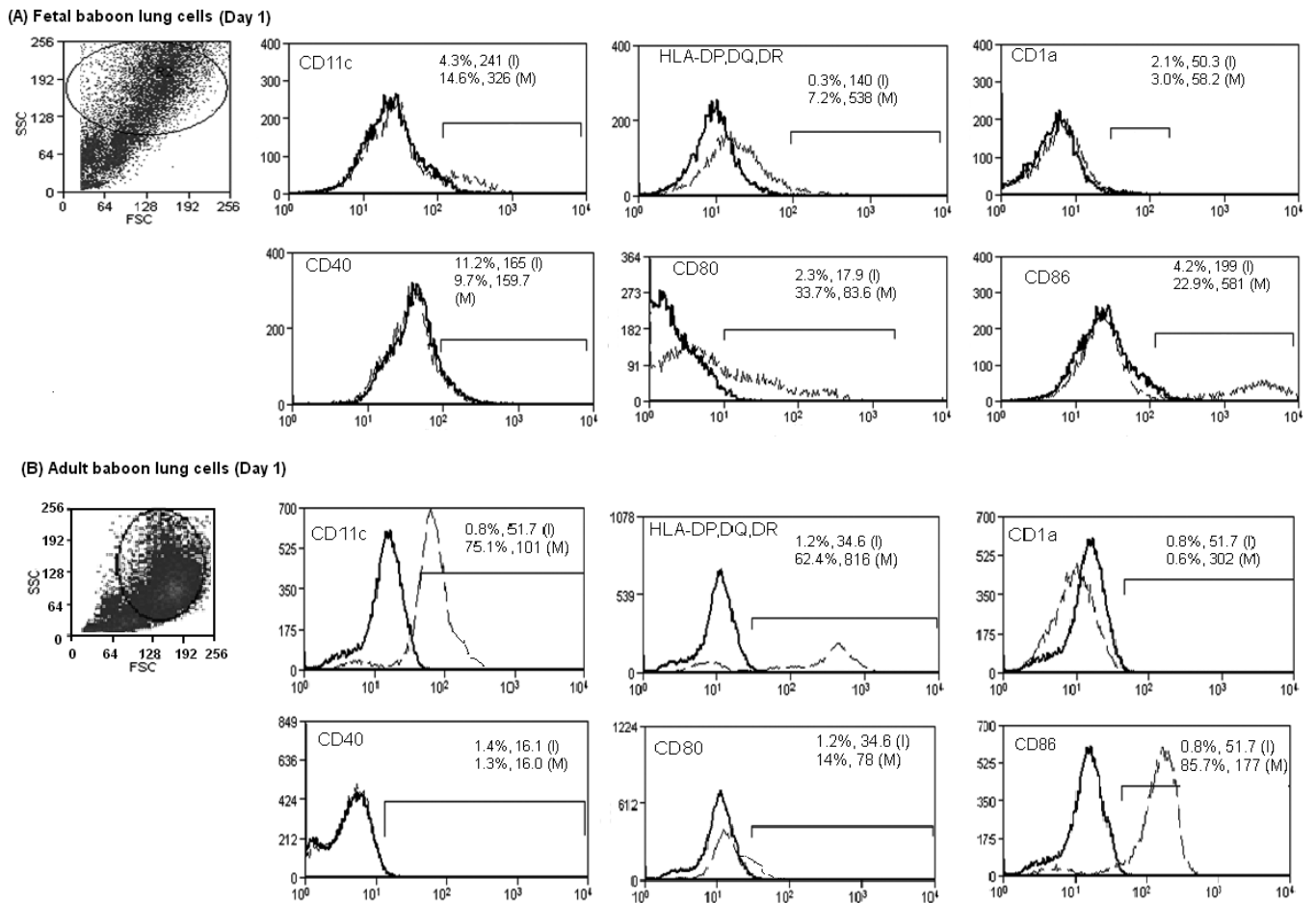


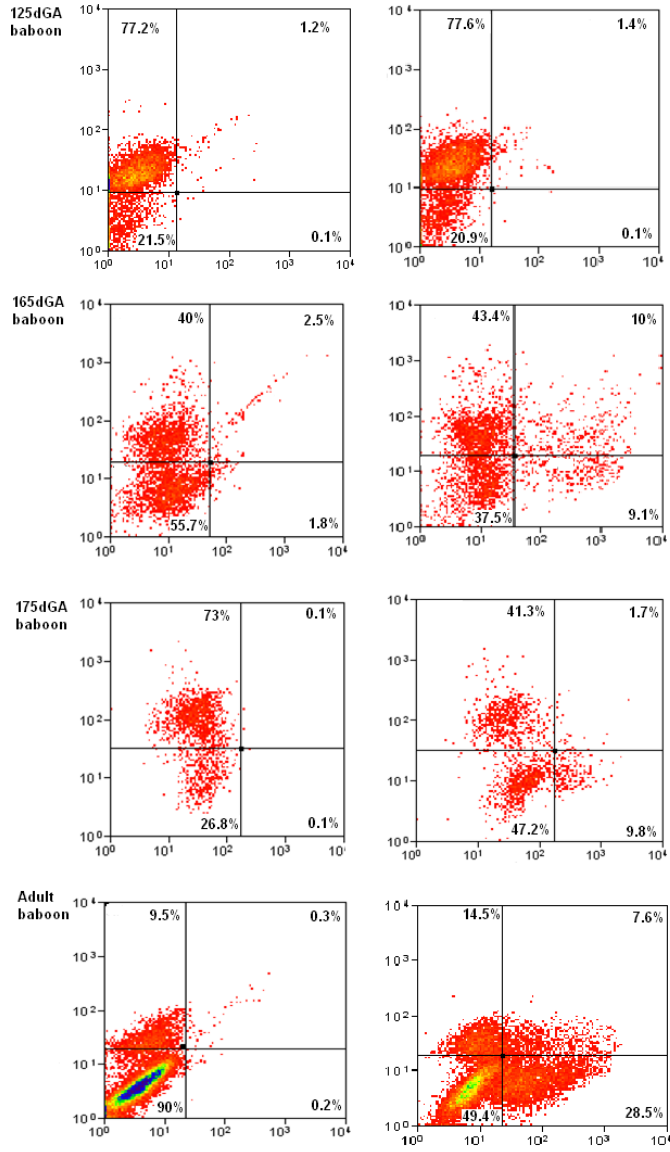
Figure 2.

FACS dot-plot and histogram charts of CD2 (T lymphocyte marker), CD20 (B lymphocyte marker) and CD14 (macrophage, monocyte marker)-antibody-stained adult baboon lung DCs collected from the top fraction of density gradient. The lung DCs were stained with fluorochrome-conjugated antibodies for CD2, CD20, CD11c and CD14 markers. The lung DCs were gated in region R (A) and the FACS dot-plot charts (B, C) were plotted to show negative staining for CD2, CD20 and CD14. Percent numbers of cells positive and MFI values for CD2 (D), CD20 (E) and CD14 (F) markers are shown within the histogram charts for isotype control antibody-stained (I) and marker-specific antibody stained (M) cells under marked area. The unstained cells showed histogram pattern similar to isotype control antibody-stained cells. Similar to adult baboon lung DCs, the fetal baboon lung cells collected from the top fraction of density gradient did not stain with CD2-, CD20- and CD14-specific antibodies.

**Figure 3.**

Flow cytometric histogram charts of fetal (A) and adult (B) baboon lung cells obtained from the top fraction of density gradient solution on Day 1. The cells with large forward and side scatter were gated within the circle. The dark line shows the histogram for isotype control antibody-stained cells, and the light line shows the histogram for marker-specific antibody-stained cells. The histogram of unstained cells always showed pattern similar to the histogram of isotype control antibody-stained cells. Data on x-axis shows the fluorescence intensity. Percent numbers of cells positive and MFI values for the specific marker are shown within the histogram charts for the isotype control antibody stained (I) and marker-specific antibody stained (M) cells under marked area (). The area was selected based on absence of fluorescence by isotype control antibody-stained cells and unstained cells.

(A) Phagocytosis assay performed on ice (B) Phagocytosis assay performed at 37°C



(C) Fluorescence microphotograph showing a cell with ingested *E. coli* bioparticles

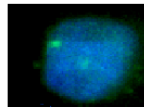


Figure 4.

Phagocytosis of *E. coli* K12 bioparticles by fetal and adult baboon lung DCs. The lung DCs from fetal (125–140dGA, n = 3; 165dGA, n = 3), close-to-term (175dGA, n = 3) and adult (n = 3) baboons were incubated with serum-opsonized, heat-killed, FITC-labeled *E. coli* bioparticles at 37°C. The cells with ingested FITC-labeled *E. coli* bioparticles show green fluorescence and collected on FL-1 channel (on x-axis). The fluorescence of cells with surface-adhered extracellular bioparticles (quenched with trypan blue) was collected on FL-3 channel (on y axis). The cells with ingested (right lower quadrant), adhered + ingested

(right upper quadrant), adhered (left upper quadrant) *E.coli* bioparticles were analyzed by Flow cytometry. Panel (A) shows the dot plot charts of lung DCs incubated with *E. coli* bioparticles on ice (negative control) and panel (B) shows the dot plot charts of lung DCs incubated with *E.coli* bioparticles at 37°C (phagocytosis or ingestion). Dot plot charts are from one representative animal of each type. The percent numbers of cells in each quadrant are shown within the dot plot charts. Panel (C) shows the fluorescent micrograph of a representative cell (stained blue with Hoechst 33342 stain) with ingested FITC-labeled *E. coli* bioparticle (green fluorescence).

Table 1

Percent fetal and adult baboon lung cells obtained from top, middle and bottom fractions after density gradient separation.

Fractions of Optiprep density gradient	*Percent cells (harvested on Day 0 and Day 1) per total lung cell number			
	Fetal Baboon		Adult Baboon	
	Day 0	Day 1	Day 0	Day 1
Top fraction	0.9 (0.2)	0.5 (0.04)	0.8 (0.5)	0.3 (0.2)
Middle fraction	6.7 (0.2)	2.5 (0.5)	4.8 (0.8)	4.3 (0.3)
Bottom fraction	92.4 (0.4)	97.0 (0.5)	94.4 (1.3)	95.4 (0.5)

* The values are mean (SEM) percent number of total lung cells from 125–165dGA fetal (n = 3) and adult (n = 4) baboons. The cells were subjected to density gradient separation either immediately (Day 0) or after overnight culture (Day 1).

Table 2

Percent numbers of cell-surface marker positive lung cells harvested in top fraction of density gradient tube after overnight culture (Day 1).

*Lung cells from top fraction			
Cell-surface marker	125–140dGA Baboon	175dGA Baboon	Adult Baboon (10–35 years age)
CD11c	5.8 (4.2)	2.8 (0.9)	11.4 (3.8)
HLA-DP, DQ, DR	5.5 (1.5)	8.0 (2.0)	34.4 (9.2)
CD40	0.7 (0.7)	0.3 (0.1)	4.7 (2.3)
CD80	18.0 (13.1)	2.3 (1.1)	9.0 (6.5)
CD86	10.8 (7.3)	13.0 (5.0)	31.6 (9.5)

* The values are mean (SEM) percent positive lung DCs from 125–140dGA (n = 3), 175dGA (n = 3) and adult (n = 4) baboons. The isolated cells were negative for plasmacytoid DC markers- DC-SIGN (CD209), ILT7 and CMKLR1. There was no change in percent numbers of cell-surface marker positive lung cells isolated on day 0 or day 1.

Table 3Phagocytosis of *E.coli* K12 bioparticles by fetal and adult baboon lung DCs.

Baboons* →	Mean percent cells (SEM)			
	125–140dGA	165dGA	175dGA	Adult (10–35 years age)
Ingestion	0.1 (0.0) [†]	1.7 (1.6) [†]	5.1 (2.7) [†]	17.7 (5.8)
Ingestion + adherence	0.4 (0.0) [†]	3.4 (0.2) [†]	1.6 (0.3) [†]	5.8 (0.0)
Adherence	83.6 (0.0) [†]	62.2 (1.3) [†]	67.5 (9.9) [†]	21.0 (0.0)
No interaction	15.9 (0.0) [†]	32.7 (2.8)	25.9 (7.1) [†]	62.0 (8.4)

*The results are from 125–140dGA (n = 3), 165dGA (n = 3), 175dGA (n = 3), and adult (n = 4) baboons.

[†]p<0.05 versus adult baboon.

Author Manuscript

Author Manuscript

Author Manuscript

Author Manuscript